**Published online November 18, 2004**

*Nucleic Acids Research, 2004, Vol. 32, No. 20* ***1–12***
*doi:10.1093/nar/gkh939*

# Regulation of 6S RNA biogenesis by switching utilization of both sigma factors and endoribonucleases

**Kwang-sun Kim and Younghoon Lee***

Department of Chemistry and Center for Molecular Design and Synthesis, Korea Advanced Institute of Science and Technology, Daejeon 305-701, Korea

Received August 4, 2004; Revised and Accepted October 26, 2004

## ABSTRACT

**In *Escherichia coli*, 6S RNA functions as a modulator of RNA polymerase $\sigma^{70}$-holoenzyme activity, but its biosynthetic pathway remains uncharacterized. In this study, to further understand the regulatory circuit of 6S RNA biosynthesis for the modulation of E$\sigma^{70}$ activity, we have characterized the biogenesis of 6S RNA. We reveal that there are two different precursors, a long and a short molecule, which are transcribed from the distal P2 and proximal P1 promoter, respectively. Transcription from the P2 promoter is both $\sigma^{70}$- and $\sigma^{S}$-dependent, whereas, in contrast, P1 transcription is $\sigma^{70}$- but not $\sigma^{S}$-dependent. Both precursors are processed to generate the 5′ end of 6S RNA, and while the long precursor is processed exclusively by RNase E, the short precursor is processed by both RNase G and RNase E. Our data indicate that the switching of the utilization of both sigma factors and endoribonucleases in the biogenesis of 6S RNA would play an essential role in modulating its levels in *E.coli*.**

## INTRODUCTION

Small non-coding RNAs (sRNAs) ranging from 40 to 500 nt in size are involved in a number of cellular processes in bacteria, such as transcription, RNA processing, messenger RNA (mRNA) turnover, translation, protein degradation and secretion (1–4). sRNA molecules are generally transcribed as longer precursor products of RNA polymerase (RNAP) which then undergo a series of processing reactions to remove extra residues at either the 5′− and/or 3′ ends by various ribonucleases to generate the mature, functional forms (5). Although the biogenesis of rRNA and transfer RNA (tRNA) has been extensively studied (6,7), relatively little is yet known about the synthesis of other sRNA types. Nonetheless, the biogenesis of some sRNAs is now well characterized, such as M1 RNA, the catalytic subunit of the RNase P (8,9). M1 RNA is transcribed from the *rnpB* gene as a precursor molecule (10–12) and eventually formed through a processing event involving RNase E and exoribonucleases (13–16). Another well-characterized example is tmRNA, which is involved in removing products translated from truncated mRNAs (17). tmRNA is transcribed from the *ssrA* gene and the primary transcript is processed to generate mature tmRNA. This processing reaction requires endoribonucleolytic cleavages by RNase P, RNase III and RNase E, followed by exoribonucleolytic trimming (14,18–20).

6S RNA, an sRNA molecule, was initially identified by polyacrylamide gel analysis of *in vivo* labeled total RNA (21). Its abundance in the *Escherichia coli* genome was estimated to be 1000–1500 molecules, which is ~25% of the total number of ribosomes (22). 6S RNA does not associate with ribosomes, but appears to be complexed with a number of proteins and migrate at about 11S (22). Functional studies of 6S RNA had, however, originally been hampered by the lack of a detectable phenotype for either 6S RNA null mutants (23) or 6S RNA overexpressing cells (24). It was eventually discovered that 6S RNA specifically interacts to the majority of RNAP $\sigma^{70}$-holoenzyme (E$\sigma^{70}$) and reduces its activity, making it possible to alter the utilization of E$\sigma^{70}$ to E$\sigma^{S}$ in cells following their transition into the stationary phase of growth (25). Furthermore, a recent study on growth phenotypes of 6S RNA-deficient cells suggests that 6S RNA is required for long-term cell survival (26). The fact that 6S RNA accumulates throughout cell growth (25) also suggests that it may mediate growth-dependent changes in the physical properties of RNAP.

A precursor 6S RNA, with six to eight additional bases at the 5′ terminus, was described previously (27), indicating that 6S RNA is derived from a larger primary transcript. In addition, 6S RNA is transcribed from the *ssrS* gene as part of a dicistronic message containing an open reading frame (ORF) (*ygfA*) at the 3′ end (24). However, the *ssrS* gene promoter has not been well characterized. Furthermore, the maturation mechanism of 6S RNA from its precursor has not been elucidated, except that a plausible 3′ trimming mechanism has been hypothesized (14). Given that 6S RNA functions as a regulator of the modulation of E$\sigma^{70}$ activity, the biogenesis of 6S RNA should be regulated according to the requirements for E$\sigma^{70}$ activity. However, the mechanisms underlying this regulation remain obscure, mainly due to the lack of knowledge of 6S RNA biosynthesis.

Our present study was therefore designed to determine the mechanism of 6S RNA synthesis in *E.coli* and the association

*To whom correspondence should be addressed. Tel: +82 42 869 2832; Fax: +82 42 869 2810; Email: Younghoon.Lee@kaist.ac.kr

of this biosynthetic pathway with the regulatory circuits required for the modulation of transcription, in response to a change in growth conditions. We show that two 6S RNA precursors are generated and that they are transcribed from two tandem promoters. A longer precursor is transcribed from a distal $\sigma^S$-dependent promoter, P2, and is then processed exclusively by RNase E, whereas the shorter precursor is expressed via a proximal $\sigma^{70}$-dependent promoter, P1, and is processed by both RNase E and RNase G. The findings of this study indicate that the modulation of the cellular levels of 6S RNA during cell growth could be accomplished through the coordination of both transcriptional and post-transcriptional regulation by switching the utilization of sigma factors and endoribonucleases.

## MATERIALS AND METHODS

### Bacterial strains

*E.coli* K-12 strain JM109 was used for the construction of plasmids. Strains GW11 (W3110 but *cafA::cat*), GW20 (W3110 but *ams1*), and GW21 (the same as GW20 but *cafA::cat*) were kindly provided by Dr Wachi, and SK7622 (MG1693 but Δ*rnc-38 Km*$^r$) was provided by Dr Kushner (28,29). Strain W3110 or MG1693 was used as wild-type controls. A *rpoS*$^-$ strain, KS1000 (*rpoS*::*km*), was constructed in a W3110 background by inserting the kanamycin resistance gene (*km*$^R$) into codon 53 of *rpoS* as described previously (30,31). Briefly, a kanamycin cassette was amplified by PCR from *Tn5* using primers ***km1*** (5′ TAT GGA CAG CAA GCG AAC CG) and ***km2*** (5′ TCA GAA GAA CTC GTC AAG AAG). Then, a recombinant cassette (*km-rpoS*) was constructed by PCR using the kanamycin cassette as a template with primers ***km-rpo1*** (5′ GAT AAC GAT TTG GCC GAA GAG GAA CTG TTA TCG CAG GGA GCC ACA CAG CGA TGG ACA GCA AGC GAA CCG) and ***km-rpo2*** (5′ CTT CTT GAC GAG TTC TTC TGA TGT GTT GGA CGC GAC TCA GCT TTA CCT TGG TGA GAT TGG TTA TTC ACC ACT). The resulting PCR product was directly introduced into strain DY330 (30) by electroporation. Recombinants were selected as *km*$^R$ clones and were confirmed by PCR with *rpoS*-specific primers (5′ GTA GAA CAG GAA CCC AGT GA and 5′ TAC GGG TTT GGT TCA TAA TC). The defective prophage in the recombinant was removed as described in the method by Yu *et al*. (30) to generate strain KS330. Bacteriophage P1-mediated transduction was used to construct KS1000 (*rpoS::km*) by employing W3110 (wild type) as the recipient strain, and KS330 as the donor strain. KS1000 was confirmed by sequencing the PCR product amplified with the *rpoS*-specific primers.

### Preparation of total cellular RNA

*E.coli* cultures were grown overnight in Luria–Bertani (LB) broth and diluted 1:100 in the same medium and grown further to an $OD_{600}$ of 0.5 at 30°C. In the case of *rne*$^{ts}$ cells, the cells were grown at 30°C to an $OD_{600}$ of 0.5, and then shifted to 44°C for 1 h before RNA preparation. For RNA preparation from cells at a specific stage of growth, *E.coli* cells grown overnight were diluted 1:100 in LB broth and continued to be grown at 37°C. Aliquots of the cell culture were taken at intervals. Total cellular RNA was isolated by hot phenol extraction as described previously (13). To remove contaminating DNA, DNA-free™ (Ambion) was added to the RNA samples according to the manufacturer's instructions. RNA isolates were further cleaned up using an RNeasy® Mini Kit (Qiagen).

### Northern blot analysis

Total cellular RNA extracts of 30 μg were fractionated on a 5% polyacrylamide gel containing 7 M urea and electrotransferred onto a Hybond-N+ membrane (Amersham Pharmacia). To construct plasmid pKS200, a template DNA generating an antisense 6S RNA probe, an *ssrS* DNA fragment between −3 and +197, was amplified by PCR and cloned into the HindIII/BamHI site of pGEM3. For the preparation of the antisense 6S RNA probe, the HindIII-digested pKS200 was used as a template for *in vitro* transcription with T7 RNAP. *In vitro* transcripts were labeled internally with [α-$^{32}$P]CTP. Oligonucleotides anti-5S (5′ CGG CAT GGG GTC AGG TGG) and anti-rnaI (5′ GTG GTT TGT TTG CCG GAT) were labeled at the 5′ end with [γ-$^{32}$P]ATP and polynucleotide kinase, and they were used as probes for 5S RNA and RNA I, respectively. Hybridization was performed as described previously (13). Quantitative analysis of hybridization signals was performed using an Image Analyzer BAS1500 (Fuji).

### RACE assays

5′ RACE (rapid amplification of cDNA ends) analysis was carried out as described previously (32), with minor modifications. Briefly, 1 μg of total cellular RNA was treated with 1 U of tobacco acid pyrophosphatase (TAP) in a 50 μl reaction. The TAP-treated RNA was then ligated with 500 pmol of A3 (32), as a 5′ adaptor RNA, at 15°C for 16 h with 50 U of T4 RNA ligase (New England Biolabs) in a 50 μl reaction. Adaptor-ligated RNA was then reverse transcribed and PCR amplified using a Titan One-Tube RT–PCR kit (Roche Applied Science) according to the manufacturer's instructions. PCR products were separated on a 3% agarose gel and purified by gel elution. They were analyzed by DNA sequencing after cloning into a pGEM-T-easy vector (Promega). 3′ RACE analysis was carried out identically to 5′ RACE analysis except that total cellular RNA (1 μg) was first dephosphorylated with 0.01 U of calf intestine alkaline phosphatase (Promega) in a 50 μl reaction, ligated with E1 3′ adaptor RNA (32).

### Primer extension analysis

To identify the 5′ ends of 6S RNA transcripts, primer extension analysis was performed using primer ***a*** (5′ TTC TTG TGG TAT GAA ATA TCG G) and primer ***b*** (5′ ACT TGC CGC GTA GTC ACG AGT). Primer ***cat*** (5′ ACG GTG GTA TAT CCA GTG AT) was used to analyze *ssrS-CAT* fusion transcripts. These primers were labeled with [γ-$^{32}$P]ATP at the 5′ end with T4 polynucleotide kinase, and total cellular RNA (30 μg) was annealed to 2 pmol of each labeled primer in a 25 μl reaction with four subsequent incubation steps: at 70°C for 5 min, 42°C for 20 min, 25°C for 1 h and on ice for 10 min. The primer extension reactions were performed at 42°C for 90 min according to the manufacturer's instructions with 20 U of AMV-RT (Promega) and a dNTP mixture (0.5 mM each).

The resulting products were then analyzed on an 8% denaturing polyacrylamide gel. Quantitative analysis was performed using an Image Analyzer BAS1500 (Fuji).

### S1 nuclease mapping

S1 nuclease mapping was performed essentially as described previously (33). Briefly, for the preparation of the DNA probe, plasmid pKS840, which was constructed by cloning an PCR-amplified *ssrS* DNA fragment between −420 and +420 into the HindIII/BamHI site of pGEM3, was digested with SphI and labeled at the 3′ end with [α-$^{32}$P]ddATP (Amersham Pharmacia) by terminal transferase (Roche Applied Science) according to the manufacturer's instructions. The labeled DNA was then digested with EcoRI, and a 330 bp SphI–EcoRI DNA fragment (corresponding to +88 to +418 of *ssrS*) was gel purified and this 3′ end-labeled DNA probe (0.2 pmol) and total cellular RNA (50 μg) were hybridized in 30 μl of S1 hybridization buffer (40 mM PIPES, pH 7.5, 1 mM EDTA, 0.4 M NaCl and 80% formamide). The hybridized RNA was subsequently treated with 300 U of S1 nuclease (Promega) and analyzed on an 8% polyacrylamide sequencing gel.

### *In vivo* promoter assay

Promoter-containing DNA fragments were obtained by PCR from genomic DNA with the primer pairs ***SSR1A/SSR1B*** and ***SSR2A/SSR2B***: ***SSR1A***, 5′ AGA CTC GTG ACT ACG CGG CAA; ***SSR1B***, 5′ CCC AAG CTT TGA AAT ATC GGC TCA GGG GAC; ***SSR2A***, 5′ CGC GGA TCC GCC GTT CAC TGC GTG TGA ACT; ***SSR2B***, 5′ CCC AAG CTT TTT GCT TTT TCT TGC GCT AAC. The resulting PCR products were co-digested with BamHI and HindIII and ligated into pKK232-8 (Amersham Pharmacia) to generate the *ssrS*-CAT fusion plasmids pSSR1and pSSR2, respectively. The overnight culture of JM109 cells containing the *ssrS*-CAT fusion plasmids was diluted to 1:300 in LB supplemented with ampicillin (50 μg/ml) followed by the addition of different concentrations of chloramphenicol. Following a 3 h incubation at 37°C, the $OD_{600}$ of the cultures was measured to assess cell growth inhibition and used to determine the concentration of chloramphenicol required for the 50% inhibition of the growth ($IC_{50}$) of cells as described previously (34). Alternatively, total cellular RNA was isolated from the exponentially growing JM109 cells and subjected to primer extension analysis as described above.

### *In vitro* transcription by *E.coli* polymerase

The DNA templates were constructed by replacing the *rnpB* promoter, containing a HindIII–EcoRI fragment, in pLMd23-wt (35) with the *ssrS* promoter-containing DNA fragments. The promoter-containing DNA products were obtained by PCR with primer pairs ***SSRP1f/SSRP1r*** for P1, and ***SSRP2f/SSRP2r*** for P2: ***SSRP1f***, 5′ CGC GGA TCC ACT AAC CAA AAC TTT GAA TG; ***SRP1r***, 5′ CGC GGA TCC AGG GAT GCG TTG AAT CAG GC; ***SSRP2f***, 5′ CAA GGG AAG CTT GAA TCT GCC GAG ATG CCG C; ***SSRP2r***, 5′ CAA GGG AAG CTT GAA TCT CCG AGA TGC CGC CGC. The PCR products were then digested with HindIII and EcoRI, and cloned into the HindIII–EcoRI site of pLMd23-wt to generate the pKSP series of constructs. To knock-out the promoter activity, the −10 region of P1 and P2 was changed from 'TAGAGT' to 'CTCGAG' by a site-directed mutagenesis kit (Stratagene) using primer pairs ***P1mu/P1md*** for P1 and ***P2mu/P2md*** for P2: ***P1mu***, 5′ GGT TTA CTG TGG CTC GAG AAC CGT GAA GAC; ***P1md***, 5′ GTC TTC ACG GTT CTC GAG CCA CAG TAA ACC; ***P2mu***, 5′ CTG AAA GAA CGC ACC TCG AGC ACA AAT ACT GAA C; ***P2md***, 5′ GTT CAG TAT TTG TGC TCG AGG TGC GTT CTT TCA G. *In vitro* transcription, using *E.coli* RNAP, was carried out basically as described previously (36). Briefly, the RNAP $\sigma^{70}$-holoenzyme ($E\sigma^{70}$) and the core enzyme were purchased from Ambion, and $\sigma^s$ was a gift from Dr Gutierrez. $E\sigma^s$ was reconstructed by combining the core enzyme and $\sigma^s$ in a ratio of 1:5. RNAP (4 nM) was incubated at 37°C for 30 min in reaction buffer (40 mM Tris–HCl, pH 8.0, 10 mM $MgCl_2$, 5 mM DTT, 50 mM KCl, 50 μg/ml BSA) with 3 nM of template DNA. RNAP and DNA were preincubated for 15 min, and the reaction was started by adding rNTP mixtures (200 μM of ATP, GTP, and UTP, and 20 μM of CTP including 5 μCi of [α-$^{32}$P]CTP). After 30 min, reactions were terminated by the addition of a 0.2 vol of 0.2 M EDTA in 40% glycerol with dyes. The products were analyzed on a 5% polyacrylamide sequencing gel and quantitated by BAS1500 (Fuji).

### Preparation of RNA substrates

For the preparation of RNA substrates to be used in *in vitro* processing assays, the *ssrS* regions of −221 to +285 and −9 to +285 were PCR amplified. The PCR fragments were then cloned into pGEM3 to generate the constructs pSP6SP2 and pSP6SP1. The pSP6SP2 and pSP6SP1 constructs were mutagenized with the QuikChange® (Stratagene) kit so that *in vitro* transcription would be initiated at positions −221 and −9, respectively, and generate run-off transcripts having a 3′ end at position +191 when the mutagenized plasmids were cleaved with SmaI. The resulting plasmids pKS221 and pKS9 were digested by SmaI. The DNA template for RNA I was obtained by PCR from pKK232-8 with a pair of primers ***5′SP-RNAI*** and ***3′RNAI***: ***5′SP-RNAI***, 5′-GCA TCC TAA TAC GAC TCA CTA TAG GGA CAG TAT TTG GT; ***3′RNAI***, 5′-AAC AAA AAA CCA CGC TAC CAC CAG C from pKK232-8. *In vitro* transcription was carried out using SP6 RNAP. When required, *in vitro* transcripts were internally labeled with [α-$^{32}$P]CTP, 5′-labeled with [γ-$^{32}$P]ATP and polynucleotide kinase, or 3′-labeled with [$^{32}$P]pCp and T4 RNA ligase, as described previously (37).

### *In vitro* processing reactions

N-terminal catalytic half of RNase E (NTH-RNase E) and full-length RNase G were purified as his-tagged fusion proteins to homogeneity from *E.coli* containing pNRNE or pRNG as described previously (16). RNA substrates were incubated with either NTH-RNase E or RNase G in 50 μl of reaction buffer [20 mM Tris–HCl, pH 7.5, 100 mM NaCl, 10 mM $MgCl_2$, 0.1% (v/v) Triton X-100, 1 mM DTT and 20 U RNasin (Promega)] at 37°C. These reactions were quenched with phenol/chloroform, and the products were analyzed on polyacrylamide sequencing gels and quantitated by BAS1500 (Fuji). Alternatively, the reaction products were analyzed by primer extension with primer ***a*** as described above.

## RESULTS

### Involvement of RNase E in the processing of 6S RNA transcripts

Since the processing of primary transcripts for sRNAs is generally initiated by endoribonucleases (13,15,18,38), we examined whether 6S RNA biosynthesis would be disrupted in RNase E-, RNase III- and RNase G-deficient *E.coli* strains. We analyzed 6S RNA transcript levels by northern blotting (Figure 1) and observed two major bands (***b*** and ***c***) and one minor band (***a***) in each strain including wild type. Band ***a*** was found to predominantly accumulate in RNase E-deficient cells (*rne*$^{ts}$ cells at 44°C), suggesting the involvement of RNase E in the processing of 6S RNA. In addition, we detected two minor bands between bands ***a*** and ***b*** in RNase-deficient cells.

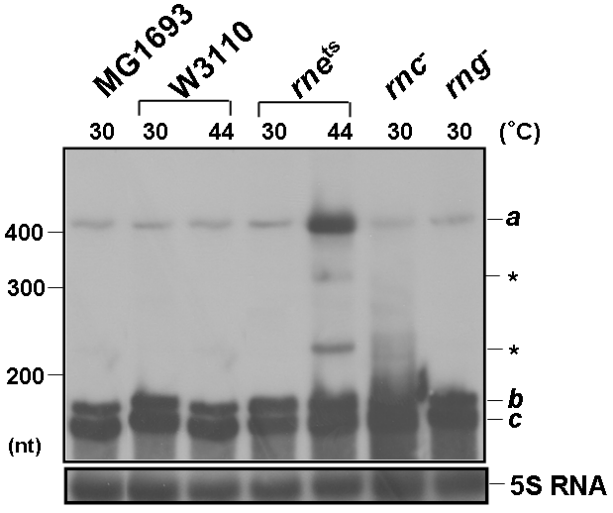


**Figure 1.** Biosynthesis of 6S RNA in cells lacking either RNase E, RNase III or RNase G. Total cellular RNA isolates were prepared from strains MG1693 (wild type), W3110 (wild type), GW20 (*rne*$^{ts}$), SK7622 (*rnc*$^{-}$) and GW11 (*rng*$^{-}$) grown to an $OD_{600}$ of ~0.4. Each RNA sample (30 µg) was fractionated on a 5% polyacrylamide gel containing 7 M urea. *In vivo* 6S RNA transcripts were analyzed by northern blotting. The different strains and the respective growth temperatures are indicated above each lane. The RNA size markers, RNA Century$^{TM}$-plus (Ambion) were used. 6S RNA transcripts are indicated as bands ***a***, ***b***, ***c*** and asterisks. Antisense 5S RNA was also used as a probe with the same membrane.

### Identification of different 6S RNA transcripts

To further identify the different 6S RNA species that are expressed in *E.coli*, we first identified their 5′ and 3′ ends using RACE assays. For 5′ RACE, total RNA isolates prepared from wild-type and RNase-deficient cells were treated with pyrophosphatase to convert any 5′-triphosphosphoryl groups to 5′-monophosphoryl groups. The treated RNA samples were then ligated with a 5′ adaptor, amplified by RT–PCR and the resulting PCR products were then analyzed on an agarose gel (Figure 2). Two bands, ***e*** and ***f***, were detectable at comparable levels in each of the strains, whereas band ***d*** was observed only in *rne*$^{ts}$ cells at 44°C (Figure 2). Each band was then eluted from the gel and subjected to DNA sequencing analysis (Table 1). The sequencing data indicated that bands ***d***, ***e*** and ***f*** were derived from 6S RNA species with 5′ ends beginning at base positions −224, −9 and −1/+1/+2, respectively. These results suggest that the mature 6S RNAs have heterogeneous 5′ ends beginning at base positions ranging from −1 to +2 and that 6S RNA precursors have 5′ ends that are transcribed from either position −224 or −9.

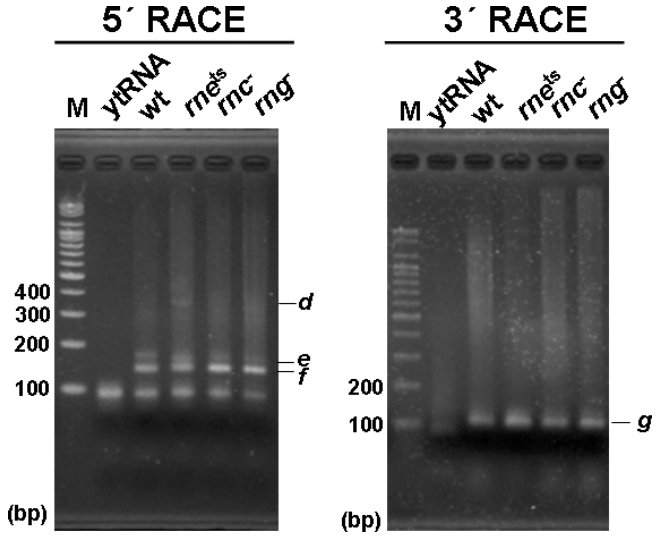


**Figure 2.** RACE products (5′ and 3′) were analyzed on a 3% agarose gel. M, 100 nt size markers; ytRNA, yeast tRNA control; wt, total cellular RNA from strain W3110 grown at 44°C; *rne*$^{ts}$, total cellular RNA from GW20 grown at 44°C; *rnc*$^{-}$, total cellular RNA from SK7622 grown at 30°C; and *rng*$^{-}$, total cellular RNA from GW11 grown at 30°C.

**Table 1.** Sequencing analysis of the RACE products

| | RACE products[a] | 5′ or 3′ ends of RNA[b,c] wt | *rne*$^{ts}$ | *rnc*$^{-}$ | *rng*$^{-}$ |
|---|---|---|---|---|---|
| 5′ RACE | ***d*** | ND[d] | −224 (5) | ND | ND |
| | ***e*** | −9 (3) | −9 (4) | −9 (4) | −9 (4) |
| | ***f*** | −1 (1), +1 (3), +2 (3) | −1 (1), +1 (3), +2 (3) | −1 (1), +1 (2), +2 (3) | −1 (1), +1 (3), +2 (2) |
| 3′ RACE | ***g*** | +184 (4), +185 (3), +186 (3) | +184 (5), +185 (2), +186 (4) | +184 (5), 185 (2), +186 (3) | +184 (4), +185 (3), +186 (3) |

[a]The RACE products shown in Figure 2 were cloned and analyzed by DNA sequencing.
[b]The 5′ or 3′ ends of 6S RNA transcripts were determined by analyzing the sequencing data of the RACE products. The numbers in parentheses indicate frequency of occurrence.
[c]RNA extracts used in the RACE assays are as follows: wt, total cellular RNA from strain W3110 grown at 44°C; *rne*$^{ts}$, total cellular RNA from GW20 grown at 44°C; *rnc*$^{-}$, total cellular RNA from SK7622 grown at 30°C; and *rng*$^{-}$, total cellular RNA from GW11 grown at 30°C.
[d]ND, not determined.

For 3′ RACE analysis, total RNA isolates were ligated to a 3′ adaptor, followed by RT–PCR amplification. Only one PCR product (band ***g***) was observed, however, in each of the strains under study and subsequent sequencing analysis of this fragment suggested that all the 6S RNA variants have heterogeneous 3′ ends that terminate at base positions ranging from +184 to +186 (Table 1). Hence, our RACE analyses suggest that two 6S RNA precursors exist with different 5′ ends that begin at either base positions −224 or −9, corresponding to bands ***a*** (long precursor) and ***b*** (short precursor) in Figure 1, respectively, and a mature 6S RNA species corresponding to band ***c***, also in Figure 1. However, we could not detect RT–PCR products corresponding to two minor bands between bands ***a*** and ***b*** shown in Figure 1, which we suspected to be due to their low concentration. We predict that these RNA species are processing intermediates derived from the long 6S RNA precursor, as there are no promoter homologies near their predicted 5′ ends (see below).

To further confirm the position of the 5′ and 3′ ends of the 6S RNA species, primer extension and S1 mapping analyses were performed using total cellular RNAs that were prepared from both wild-type and RNase-deficient cells. For 5′ end mapping of the short and long precursor, two separate primer extension reactions were carried out with primers ***a*** and ***b***, respectively (Figure 3A). The products extended from base positions −9 and +1/+2 were observed as major bands in all the strains examined, whereas the product that was extended from the −224 position was only observed as a major fragment in the *rne*$^{ts}$ cells at 44°C. These results are consistent with our 5′ RACE data. In the primer extension experiments using primer ***a***, products that were extended to positions −216/−215 and −210 were also detected. RNA species corresponding to these products were not identified in both the northern blot analysis and the RACE experiment. Therefore, they might contain the upstream sequences only, which would be produced as processing remnants from the long precursor.

The 3′ ends of the 6S RNA transcripts were further analyzed by S1 mapping using a DNA probe labeled at position +88 of the 6S RNA sequence. The DNA probes protected from subsequent digestion were found to range in size from 97 to 104 nt in length, which corresponds to 3′ ends that terminate at positions ranging from +184 to near +191 (Figure 3B). This result is consistent with our findings in the 3′ RACE experiments except that longer ends of +187 to +191 were detected. We presumed that the longer ends might be derived from incomplete digestion of S1 nuclease. It has been previously reported that 6S RNA is produced from a dual-functional transcript, containing 6S RNA and an adjoining *ygfA* ORF (24), indicating that the 3′ ends of 6S RNA should be generated by a 3′ processing reaction. It remains to be demonstrated that how the 3′ processing occurs.

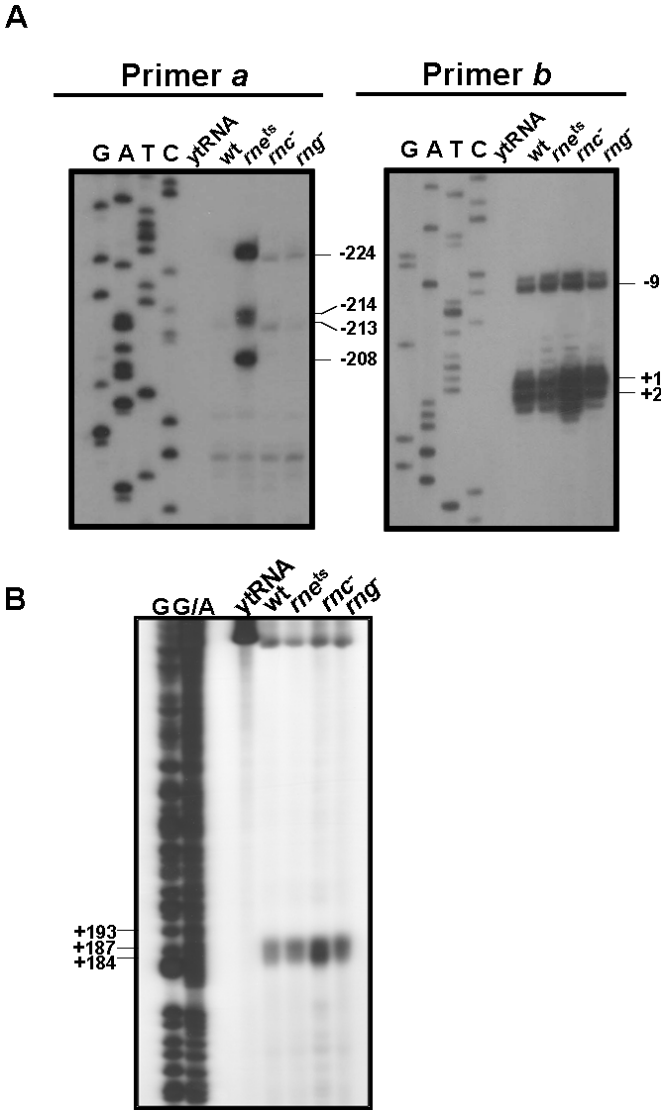


**Figure 3.** Primer extension and S1 mapping analyses. Total cellular RNA extracts were prepared from either W3110 grown at 44°C (wt), GW20 at 44°C (*rne*$^{ts}$) or SK7622 at 44°C (*rnc*$^-$), GW11 at 44°C (*rng*$^-$). Yeast tRNA (ytRNA) was used as a control. The 5′ and 3′ ends of RNA molecules were determined by primer extension analysis and S1 mapping, respectively. (**A**) Primer extension analysis. Primer extension products, generated from the $^{32}$P-labeled primer ***a*** or ***b*** (see Figure 4), were analyzed on a 5% polyacrylamide sequencing gel containing 8 M urea. G, A, T and C indicate the sequencing ladders obtained using the same primer. The positions of the 5′ ends are indicated on the right. (**B**) S1 mapping analysis. The 3′-labeled DNA probe was hybridized to total cellular RNA, and the hybrid mixture was treated with S1 nuclease and analyzed on a 5% polyacrylamide sequencing gel. G and G/A indicate G- and G/A-specific chemical reactions, respectively. The nucleotide positions of the *ssrS* gene, corresponding to G-specific cleavage products, are indicated on the left and are 1 nt smaller in length than the actual G positions.

## Characterization of transcription of the precursor 6S RNA molecules

A homology search upstream of the 5′ ends of both the short and long 6S RNA precursors for the consensus *E.coli* promoter sequence revealed two putative promoter regions, from which transcription could initiate at the 5′ end of the corresponding precursor (Figure 4). These were designated as P1 and P2, in increasing distance from the mature 6S RNA sequence. The proximal P1 region corresponds to the promoter sequence that had been previously predicted for the *ssrS* gene (24). To test whether the P1 and P2 promoters were functional *in vivo* and correctly started from the predicted sites, we subcloned DNA fragments containing these sequences upstream of the promoterless *cat* gene of plasmid pKK232-8. We then determined the concentration of chloramphenicol required for the 50% inhibition of growth ($IC_{50}$) of bacterial cells expressing these

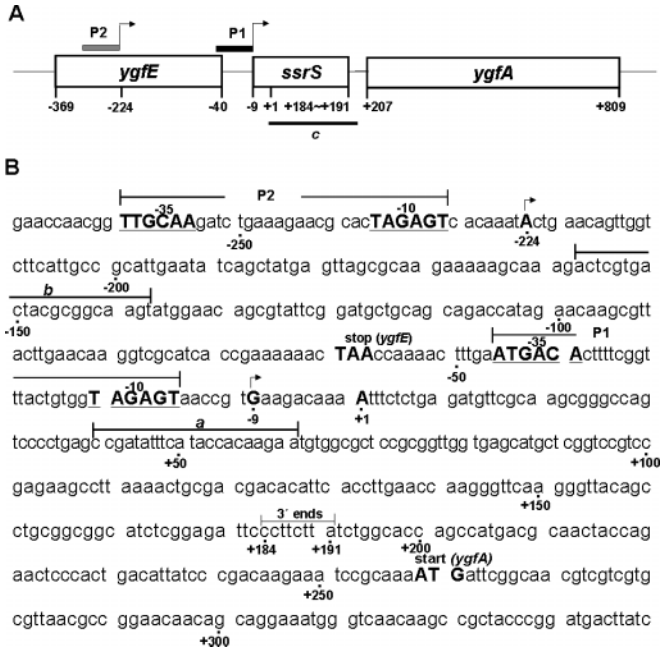


**Figure 4.** *E.coli ssrS* gene. (**A**) Schematic map of the *ssrS* transcription unit. (**B**) Nucleotide sequence of the *ssrS* gene. Promoter regions (−35 and −10) of the *ssrS* gene encoding 6S RNA are underlined, and their transcription start sites are indicated by arrows. Thick lines indicate the regions corresponding to the primers used for primer extension analysis (***a*** and ***b***) and an oligonucleotide used as the probe for northern blot analysis (***c***).

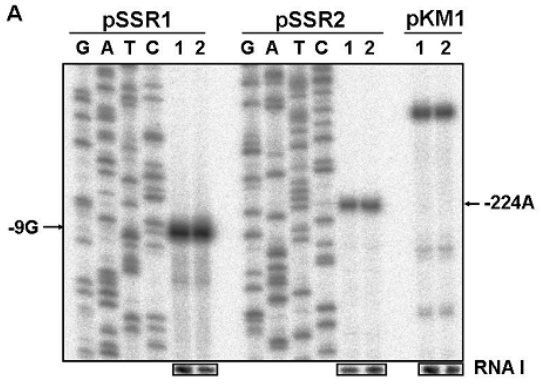


B

| | $IC_{50}$ (μg/ml) | Relative amount of transcripts |
|---|---|---|
| pKK232-8 | 30.2 ± 6.5 | N. D. |
| pKM1 | 219.6 ± 34.6 | 1.78 ± 0.44 |
| pSSR1 | 375.2 ± 41.8 | 5.62 ± 0.31 |
| pSSR2 | 158.4 ± 20.2 | 1.00 |

**Figure 5.** *In vivo* promoter activity. (**A**) Primer extension analysis of *ssrS*-CAT fusion transcripts. The regions −160 to +50 (containing P1) and −334 to −160 (containing P2) of the *ssrS* gene were cloned into pKK232-8 to generate the constructs pSSR1 and pSSR2, respectively. Plasmid pKM1, an *rnpB*-CAT fusion plasmid, was used as a control. The $^{32}$P-labeled primer (0.2 pmol) and total cellular RNA (15 μg) isolated from cells containing CAT fusion plasmids were used for each reaction. Primer extension reactions were performed in duplicate (lanes 1 and 2) for each plasmid. The relative amounts of RNA I in the total cellular RNA preparations were determined by northern blot analysis and used for assessing relative promoter activities. (**B**) Comparison of *in vivo* promoter activities. *In vivo* promoter activities were assessed by determining the concentration of chloramphenicol required for the 50% inhibition of growth of *E.coli* cells ($IC_{50}$) and calculating relative amounts of primer extension products normalized to RNA I. Plasmid pKM1, an *rnpB*-CAT fusion plasmid, was used as a control. The value represents the average of four independent experiments. N.D., not determined.

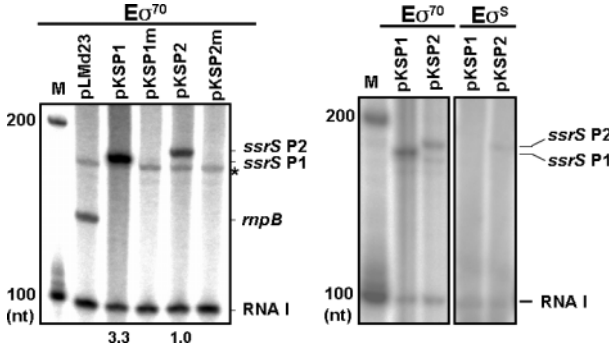


**Figure 6.** *In vitro* transcription analysis. *In vitro* transcripts generated from the *ssrS* promoter-*rnpB* terminator fusion plasmids by *E.coli* RNAP. *In vitro* transcription with either $E\sigma^{70}$ or $E\sigma^{s}$ was performed using plasmid DNAs as templates. The resulting RNA products were analyzed in a polyacrylamide sequencing gel. pKSP1, pKSP2 and pLMd23 contain the following transcription units: P1 (−109 to +90 of *ssrS*)-*rnpB*, P2 (−319 to −120 of *ssrS*)-*rnpB*, truncated *rnpB* (13), respectively. pKSP1m and pKSP2m are derivatives of pKSP1 and pKSP2, where the −10 region was mutagenized from 'TAGATG' to 'CTCGAG'. The data are representative of three independent experiments. Relative amounts of transcripts normalized to RNA I are indicated below lanes pKSP1 and pKSP2. M, size markers; asterisk, nonspecific transcripts.

constructs and performed primer extension analysis to detect *ssrS-CAT* fusion transcripts (Figure 5). Both P1 and P2 DNA fragments showed promoter activities, indicating that they are functional *in vivo*. Analysis of the *ssrS-CAT* transcripts from cells in the exponential phase grown to an $OD_{600}$ of 0.5 showed that the activity of P1 was ∼5-fold higher than the activity of P2 that was comparable to the *rnpB* promoter. Analysis of primer extension products also revealed that P1 and P2 start transcription at −9 and −224 *in vivo*, respectively.

To analyze the promoter activities of P1 and P2 *in vitro*, we replaced the *rnpB* promoter-containing DNA fragment of pLMd23-wt with the 6S RNA promoter fragments to generate P1- and P2-*rnpB* terminator transcription units. The resulting plasmid DNAs were used as templates for subsequent *in vitro* transcription assays (Figure 6). pLMd23-wt, which was used as a control, generates a 143 nt truncated *rnpB* transcript (35). If transcription initiates at −9G or −224A for P1 and P2, respectively, the sizes of the expected transcripts are 189 nt for P1 and 195 nt for P2. The P1- and P2-*rnpB* terminator units produced transcripts of the expected sizes. P1 showed an ∼3-fold higher activity than P2. When the −10 region of each promoter was mutagenized from 'TAGATG' to 'CTCGAG', both promoters no longer generated the transcripts (Figure 6). The *in vitro* transcription data, together with the *in vivo* data, indicate that the short and long 6S precursors are derived from transcription from P1 and P2, respectively. One may argue that the short precursor could be generated by processing from the long precursor. However, we conclude that the 5′ end of the short precursor is originated from the P1 transcription rather than by processing from the long precursor, because P1 is more active than P2. This conclusion is consistent with a

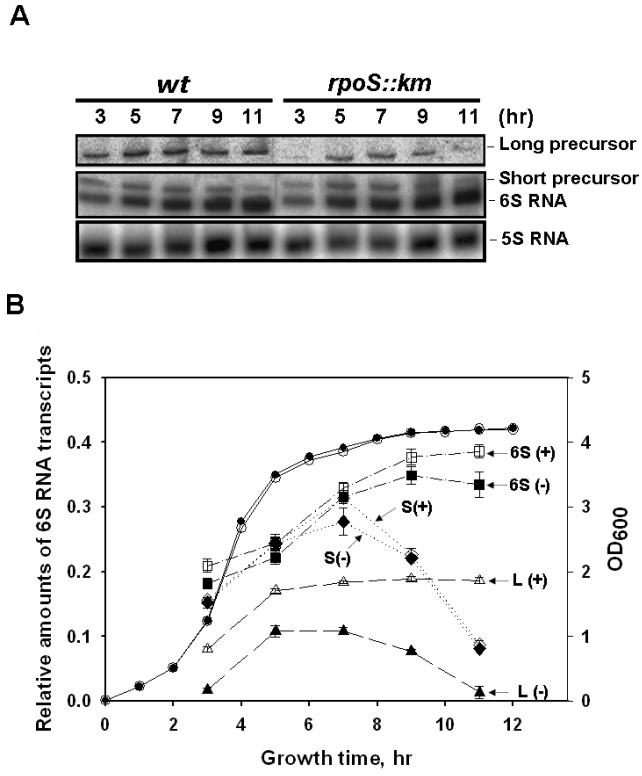


**Figure 7.** Promoter utilization in the transcription of 6S RNA. (**A**) Effect of the *rpoS* mutation on 6S RNA transcription. The W3110 (wt) and KS1000 (*rpoS::km*) strains were grown in LB medium at 37°C, and total cellular RNA extracts were prepared from cells at different growth phases and analyzed by northern blotting, as described in Figure 1. The time points at which the overnight cultures were diluted 1:100 are indicated above each lane. (**B**) Growth curves and relative amounts of 6S RNA transcripts. The relative levels of 6S RNA transcripts are represented as a ratio to 5S RNA intensities obtained by northern analysis. In the case of mature 6S RNA, however, the value is represented as one-tenth of the ratio in order to include this data in the same graph. Open and filled symbols represent *rpoS*$^+$ and *rpoS*$^-$ cells respectively. Open circle and filled circle, growth curve; Open square and filled square, mature 6S RNA (6S); open triangle and filled triangle, long precursor (L); open diamond and closed diamond, short precursor (S). +, *rpoS*$^+$ strain; −, *rpoS::km* strain. The indicated values are calculated from four independent experiments.

previous identification of a transcript carrying extra 9 nt with pppG at the 5′ end of 6S RNA (27).

The P2 promoter sequence contains a high level of homology to the consensus sequence for $\sigma^S$-dependent promoters (39–42), whereas P1 appears to be a typical $\sigma^{70}$-dependent promoter. We next determined the $\sigma^S$-dependency of transcription from the P2 promoter in strain KS1000 (*rpoS::km*), a $\sigma^S$-deficient mutant. Total cellular RNA isolates from cells at a specific stage of growth were analyzed by northern blotting for 6S RNA transcript levels (Figure 7). *rpoS*$^-$ cells generally showed lower expression of the long precursor (referred to as the P2 transcript) throughout the growth cycle than wild type. Especially, this reduction in P2 transcript levels was very dramatic in the stationary phase of growth. This result indicates that the RNAP $\sigma^S$-holoenzyme ($E\sigma^S$) produces P2 transcripts, particularly in the stationary phase. In the exponential phase of growth, P2 transcripts were still present in *rpoS*$^-$ cells, suggesting that $E\sigma^{70}$ transcribes from the P2 promoter *in vivo* as well as *in vitro*. In contrast, the levels of the short transcript (referred as the P1 transcript) were decreased at the stationary phase in both wild-type and *rpoS*$^-$ cells, indicating that P1 driven transcription is exclusively carried out by $E\sigma^{70}$. We performed additional *in vitro* transcription experiments with $E\sigma^s$ (Figure 6B, right), which was found to generate transcripts from the P2 promoter, but not P1, further confirming our finding that the P2 region is recognized by $E\sigma^s$.

### 5′ processing of 6S RNA precursors by endoribonucleases

The fact that the long 6S RNA precursor was found to accumulate in *rne*$^{ts}$ cells suggested the involvement of RNase E in the processing of 6S RNA. We therefore examined whether the long precursor was in fact cleaved by this endoribonuclease. To determine this, a substrate of 412 nt (spanning −221 to +191 of the *ssrS* gene) was synthesized *in vitro* and labeled at the 5′ ends for use in cleavage reactions with the NTH-RNase E (43–44). NTH-RNase E generated a 5′ upstream fragment by cleavage near position +1 (Figure 8A, left) leading to the generation of 6S RNA with a 5′ end at about the +1 position, which was then confirmed by an NTH-RNase E reaction with a 3′-labeled substrate (Figure 8A, right). NTH-RNase E reaction with a 3′-labeled substrate also generated 6S RNA containing extra 5 nt as a minor product. The long precursor can be digested near positions −53, −58, −62 and −66 (Figure 8A, left). As the amount of the enzyme in the reaction was increased, the initially cleaved product levels decreased with the increase of the digested products at these positions. This suggests that the digestions near positions −53, −58, −62 and −66 occurred after the initial digestion at position +1 (Figure 8A). These sites are located in A/U-rich regions, which is consistent with the previously published preferential RNase E recognition sequence (45). On the other hand, 6S RNA with a mature 5′ end was not further digested by NTH-RNase E, as shown in the reaction with the 3′-labeled substrate (Figure 8A, right).

Since RNase G is homologous to NTH-RNase E (29, 46–49), we also tested whether it would also cleave the long precursor transcript (Figure 8B). RNase G did not, however, generate mature 6S RNA, even at the highest enzyme concentrations, suggesting that it is not involved in the 5′ processing of the long precursor.

Next, the short precursor was investigated for cleavage by NTH-RNase E and RNase G, although no prominent accumulations of this precursor were observed in RNase E- and RNase G-deficient cells (Figure 1). A substrate of 200 nt (spanning −9 to +191 of *ssrS*), synthesized *in vitro*, was labeled at the 5′ end and used in the reactions (Figure 8B). In contrast to our findings with the long precursor, both enzymes were found to cleave the short precursor at comparable efficiencies. However, the cleavage site preference was slightly different between the two enzymes. RNase G cleaved preferentially at a position that was 1 nt downstream of the major cleavage site of RNase E.

The size markers (alkaline hydrolysis or G-specific fragments) used for the analysis of the reaction products had a 3′-phosphoryl group instead of a 3′-hydroxyl group generated by RNase E or RNase G. Since RNA molecules with a 3′-hydroxyl group migrate more slowly than RNA species with a

3′-phosphoryl group (50), it is difficult to determine the precise 5′ end of products with this size marker ladder. To circumvent this problem, we carried out primer extension analysis with the cleavage products (Figure 8C). The resulting data indicated that RNA with a 3′-hydroxyl group migrated at a rate that was ~1 nt slower than RNA with a 3′-phosphoryl group. Hence, we conclude that RNase E cleaves predominantly at position +1, regardless of whether the molecule is the long or short precursor, whereas RNase G cleaves the short precursor at positions 1+ and +2 with a slight preference for the +2 site.

We also compared cleavage efficiency of the long and short precursors by either NTH-RNase E or RNase G *in vitro* (Table 2). In this experiment, we used internally labeled substrates with a triphosphoryl group at their 5′ end because natural 6S RNA precursors have a 5′-triphosphoryl group as primary transcripts. We confirmed that the two RNase preparations had comparable functional purities, using RNA I as a control substrate. The cleavage rate of RNA I by NTH-RNase E

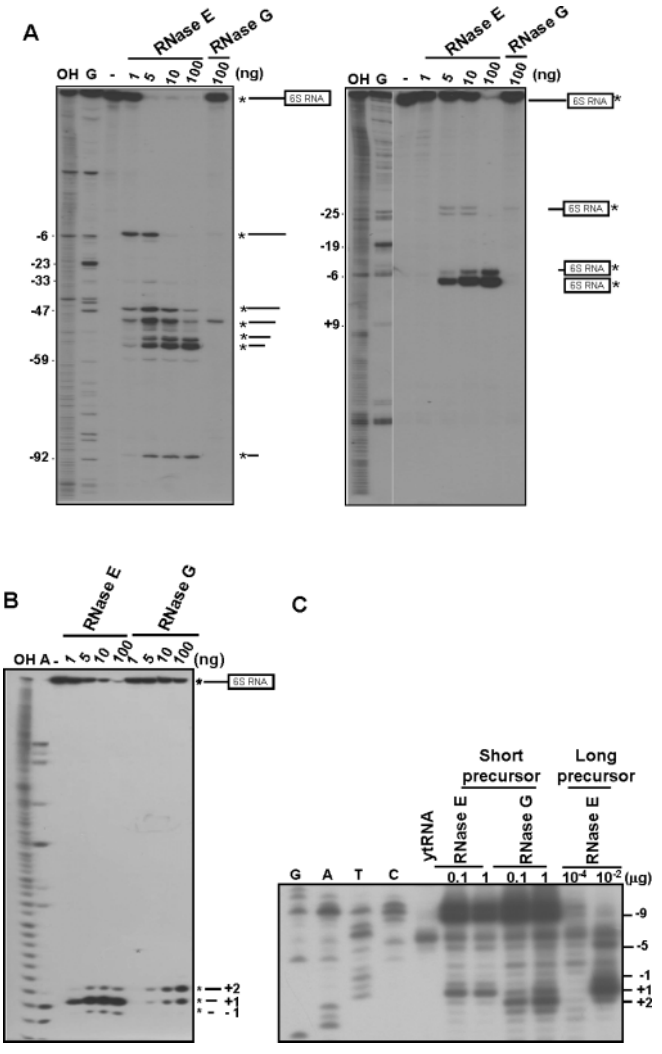


**Figure 8.** *In vitro* processing reactions. (**A**) The long 6S RNA precursor, transcribed *in vitro*, was $^{32}$P-labeled at the 5′ end (left) or 3′ end (right). It is noteworthy that the 5′-labeled substrate had a 5′-monophosphoryl group, while the 3′-labeled substrate had a 5′-triphosphoryl group. The labeled substrate was incubated with either NTH-RNase E or RNase G in a 50 μl reaction at 37°C for 10 min. The products were then analyzed on 5% polyacrylamide sequencing gels. OH, partial alkaline hydrolysis ladders; G, G-specific (RNase T1) cleavage products; −, no enzyme; asterisk, the position of label. The quantities of NTH-RNase E or RNase G used are indicated each lane. (**B**) Cleavage of the 5′-labeled short 6S RNA precursor by either NTH-RNase E or RNase G was analyzed on a 15% polyacrylamide gel, as described in (A). OH, partial alkaline hydrolysis ladders; U2, A-specific (RNase U2) cleavage products; −, no enzyme; asterisk, the position of label. The alkaline hydrolysis ladders and A-specific (RNase U2) cleavage products used as size markers have a 3′-phosphoryl group, while NTH-RNase E or RNase G cleavage products have a 3′-hydroxyl group. Since they migrate differently on the gel, the precise cleavage sites differ from the corresponding sites of the size markers up to several bases. (**C**) Assignment of the precise cleavage sites. The unlabeled substrates were cleaved with NTH-RNase E or RNase G, and cleavage sites were determined by primer extension analysis with primer *a* as in Figure 3A. The amounts of the enzymes used are indicated. All data are representative of three independent experiments.

**Table 2.** Comparison of cleavage rates of the long and short precursor 6S RNA transcripts by NTH-RNase E and/or RNase G

| Enzymes | Substrates[a] | Rate ($10^{-2}$ × pmol/min ng of protein)[b] | Relative activity |
|---|---|---|---|
| NTH-RNase E | Long precursor | 19.18 (±2.26) | 13.6 |
| | Short precursor | 1.41 (±0.64) | 1 |
| | p23 RNA | 5.28 (±0.94) | 3.7 |
| | RNA I | 6.14 (±0.84) | 4.4 |
| RNase G | Long precursor | <0.01 | 0 |
| | Short precursor | 1.19 (±0.26) | 0.84 |
| | p23 RNA | <0.01 | 0 |
| | RNA I | 1.28 (±0.42) | 0.91 |

[a]Substrates internally labeled with [α-$^{32}$P]CTP were used and therefore contained a 5′-triphosphoryl group.
[b]Rates are represented as picomole of substrates in 1 min by 1 ng of enzyme under our cleavage reaction conditions.

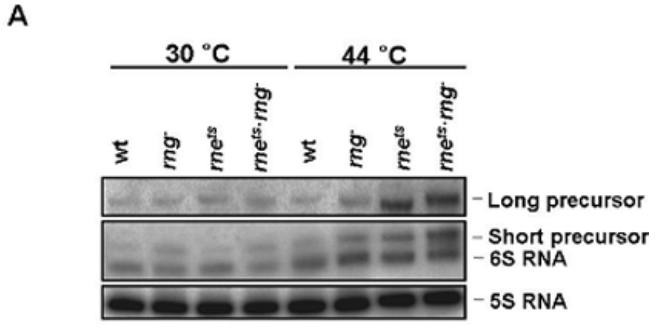


B

| Relative amount of transcripts at 44°C | | | | |
|---|---|---|---|---|
| Strains | WT | *rng* | $rne^{ts}$ | $rne^{ts}$·*rng* |
| Long precursor | 1 | 1.05 ± 0.16 | 4.16± 0.35 | 4.15± 0.40 |
| Short precursor | 1 | 1.68± 0.18 | 1.96 ± 0.27 | 3.09 ± 0.29 |

**Figure 9.** Effect of the $rne^{ts}$·$rng^{-}$ double mutation on the processing of 6S RNA. (**A**) Total cellular RNA (30 μg) was fractionated on a 5% polyacrylamide gel containing 8 M urea, and 6S RNA transcripts were analyzed by northern blot as described in Figure 1. The different strains and growth temperatures are indicated above each lane. wt, W3110; $rng^{-}$, GW11; $rne^{ts}$, GW20; $rne^{ts}$·$rng^{-}$, GW21. (**B**) The relative amount of transcripts represents the northern signal of each transcript relative to that of 5S RNA. The values were calculated from three independent experiments.

was 4.8-fold higher than that by RNase G. This difference in the cleavage rate between two enzymes is comparable to other investigators' data (51). NTH-RNase E cleaved the long precursor ~14-fold more efficiently than the short precursor, and the efficiency of short precursor processing by RNase G was similar to that by NTH-RNase E. Hence, the long precursor may contribute to the overall 6S RNA level more significantly than expected from the lower promoter activity of P2.

Our *in vitro* cleavage data (Figure 8 and Table 2) clearly showed that the long precursor is processed exclusively by RNase E, whereas the short precursor is processed by both RNase G and RNase E. To test whether this differential involvement of endoribonucleases in the 5′ processing of 6S RNA occurs *in vivo*, we examined the cellular levels of the long and short precursors in *rne*$^{ts}$, *rng*$^{-}$ and in *rne*$^{ts}$·*rng*$^{-}$ double mutant strains (Figure 9). The long precursor transcript was found to accumulate in *rne*$^{ts}$ cells, but not in *rng*$^{-}$ cells. On the other hand, the short precursor transcript accumulated primarily in *rne*$^{ts}$·*rng*$^{-}$ double mutant cells. These data suggest that the differential recognition of these two precursors by RNase E and RNase G occurs in the cell as well as *in vitro*.

## DISCUSSION

We found that *E.coli* 6S RNA is transcribed from two tandem promoters, designated P1 and P2, which are proximal and distal to the mature 6S RNA sequence, respectively. P1 is a canonical $\sigma^{70}$-dependent promoter, while P2 is both a $\sigma^{70}$- and a $\sigma^{S}$-dependent promoter. Hence, transcription of 6S RNA can be regulated by switching σ factors for the formation of specific RNAP holoenzymes, in response to environmental signals. We also found that the transcripts that are generated by these two promoters are differentially processed at their 5′ ends by RNase E and RNase G. The P2 transcript is processed exclusively by RNase E, whereas the P1 transcript is processed by both RNase E and RNase G. From these findings, we propose a working hypothesis for the biosynthetic pathways of 6S RNA (Figure 10). In this model, 6S RNA is supplied from two sources. One is the long primary precursor transcript, the expression of which is driven by the P2 promoter. The other is a short primary precursor transcript generated from the P1 promoter. Both transcripts are generated by the RNAP $\sigma^{70}$-holoenyzme ($E\sigma^{70}$) during the exponential phase of bacterial growth. In the stationary phase, however, transcription from P1 declines, presumably due to the inactivation of $E\sigma^{70}$, whereas expression from the P2 promoter region remains active via the switching from $E\sigma^{70}$ to $E\sigma^{s}$ in the RNAP holoenzyme. These primary transcripts are subjected to both 5′ and 3′ processing to generate mature 6S RNA, but the enzymes involved in 3′ processing have not been yet identified, except that final trimming requiring exoribonucleases has been reported (14). 5′ processing of 6S RNA is accomplished by both RNase E and RNase G. The short 6S RNA precursor molecule, transcribed from P1, is processed by RNase E and RNase G at the 5′ end, but the long precursor, expressed from the P2 promoter, is processed exclusively by RNase E. 5′ processing of the short precursor is also far less rapid when compared with the long precursor. Hence, these two precursor molecules differentially contribute to the synthesis of *E.coli* 6S RNA via different processing enzymes and with differing efficiencies. As a result of this biosynthetic pathway, the generation of 6S RNA can be regulated via the coupled action of sigma factors and endoribonucleases.

6S RNA levels accumulate throughout the bacterial growth cycle and, subsequently, the levels of mature 6S RNA strongly increase in the stationary phase. 6S RNA inhibits

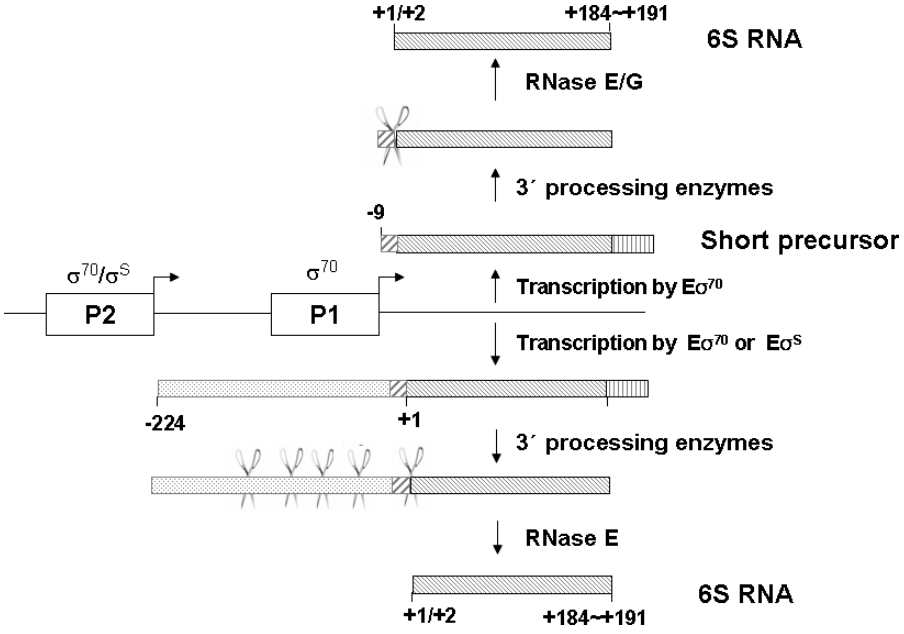


**Figure 10.** A model for the biogenesis of 6S RNA. $E\sigma^{70}$ RNAP acts during the exponential growth phase of *E.coli* for the transcription of both the long and short precursor molecules. When the cell cultures enter into the stationary phase, $E\sigma^{70}$ does not act as the major machinery to transcribe 6S RNA as $E\sigma^{S}$ now takes on this role, but only in the transcription of the long precursor. The 5′ ends of 6S RNA are formed from the short precursor by processing with either RNase E or RNase G, and from the long precursor by processing exclusively with RNase E. The processing remnant derived from the long precursor is also further cleaved by RNase E. The enzymes involved in the 3′ end formation of 6S RNA have not yet been identified, although it has now been shown that exoribonucleases are involved in final trimming (14).

the utilization of $\sigma^{70}$-dependent promoters in the stationary phase by interacting with $E\sigma^{70}$ (25). An important question, therefore, is how the transcription of 6S RNA occurs throughout the growth cycle and our findings provide a possible answer. $E\sigma^{70}$ transcribes 6S RNA from both the P1 and P2 promoters in the exponential growth phase, but it stops transcription when cells are entering the stationary phase. $E\sigma^{s}$ then takes over the control of 6S RNA transcription by recognizing the P2 promoter in the stationary phase. 6S RNA inhibits transcription from some, but not all, $\sigma^{70}$-dependent promoters, which have mostly the extended −10 sequence element as a common feature (26). The P1 promoter has the extended −10 element with the additional conserved sequence of TGG, whereas P2 does not. Therefore, P1 transcription by $E\sigma^{70}$ may be inhibited by the accumulation of 6S RNA above a specific threshold upon transition into stationary phase. If this is the case, this regulation of $E\sigma^{70}$ would be a striking example of feedback inhibition of gene expression.

Another important finding in our current study is that the two 6S RNA precursor transcripts are differently processed. The long precursor is processed exclusively by RNase E, whereas the short precursor is processed by both RNase E and RNase G. RNase G shares a high degree of homology with the N-terminal catalytic domain of RNase E (48–49). These two enzymes also share a number of common properties, such as a propensity to cleave RNA located in single-stranded regions rich in U and A nucleotides and a preference for 5′ monophosphorylated over 5′ triphosphorylated RNA substrates (51–53). However, these two enzymes may function in a distinct manner in cells because the respective deletion mutants show different cell growth effects: RNase G is dispensable for cell growth but RNase E is essential (29,47,54–56). This may be explained by a specificity difference between these two enzymes as we have found that RNase G can cleave only the short precursor despite the fact both precursors of 6S RNA contain the same consensus region for this enzyme. A possible explanation for such a specificity difference may also be that RNase G preferentially recognizes cleavage regions that are immediately proximal to the 5′ end of the precursor. The preference of RNase G for cleavage regions close to the 5′ end was previously observed for substrates, such as RNA I, *ompA* mRNA and 9S RNA (53). The limited recognition of the consensus cleavage site by RNase G may also be due to high order structures within the RNA substrates that prevent the enzyme from gaining access to this region. However, the explanation as to why RNase G, but not RNase E, is affected by these structures is still uncertain. In any case, it is likely that RNase G is not a versatile enzyme, at least with respect to substrate specificity, compared with RNase E.

The reaction rates of NTH-RNase E for the processing of *E.coli* 6S RNA long and short precursors are quite different. NTH-RNase E cleaves the long precursor much more efficiently than the short precursor, and although RNase G cleaves the short precursor, its efficiency is also much lower (Table 2). Hence, the rapid generation of 6S RNA from the long precursor molecule may be essential for the synthesis of large quantities of mature 6S RNA during the stationary growth phase where this precursor molecule is the only source of unprocessed transcripts. In addition, the difference in the processing efficiency of these two precursors can affect the supply of mature 6S RNA in other growth phases. The cellular levels of 6S RNA could therefore be post-transcriptionally controlled by the coordinate action of both RNase E and RNase G.

We showed from our current data that the 5′ end of 6S RNA is heterogeneous and that this seems to result from the cleavage of precursor 6S RNAs at multiple sites by RNase E and RNase G. Our *in vitro* experiments indicate that RNase E generates 6S RNA with 5′ ends at position +1 as the major product, −1 and +2 as minor products, and that RNase G generates 6S RNA of +1 and +2 5′ ends with a slight preference for the +2 position. However, primer extension analysis of *in vivo* RNA transcripts showed that 6S RNA molecules with 5′ ends at positions +1 and +2 are present at almost equal levels, even in RNase G-deficient cells. The discrepancy between our *in vivo* and *in vitro* data suggests that a portion of the 6S RNA molecules with a 5′ end at +1, generated by RNase E, may be further somehow digested by 1 nt *in vivo*. It is noteworthy, however, that the *in vivo* cleavage sites of RNase E, or possibly RNase G, could be changed by a cellular factor. For example, NTH-RNase E cleaves pM1 RNA with a preference for position +379 *in vitro*, but its cleavage site preference changes to position +378 in the presence of a cellular factor (16). Hence, the cleavage site preference of RNase E and RNase G may differ under *in vitro* and *in vivo* conditions. It remains to be demonstrated whether 6S RNA, with different 5′ ends, have different cellular functions or different fates during RNA metabolism.

Since 6S RNA participates in the modification of general transcription upon changes to environmental growth conditions, its cellular levels should be regulated in response to environmental signals. To gain insight into this regulation circuitry, we characterized the biosynthetic pathway of 6S RNA at both the transcriptional and post-transcriptional levels and provided a molecular basis for the regulation of 6S RNA biosynthesis. Recently, it has become apparent that sRNAs are far more abundant and have more important roles in regulatory networks, modulating various cellular processes, than previously envisaged (2–4,57,58). In many cases, sRNAs are involved in these control networks by adding another layer of regulation to the existing molecular pathways. In this respect, the finding that the biogenesis of 6S RNA is regulated by switching the utilization of both sigma factors and endoribonucleases can improve our understanding of these sRNA regulation mechanisms.

## ACKNOWLEDGEMENTS

We thank Drs M. Wachi and S.R. Kushner for providing the RNase-deficient strains, and Dr C. Gutierrez for providing the purified $\sigma^{s}$ protein. This work was supported by the 21C Frontier Microbial Genomics and Application Center Program (MG02-0201-003), the Molecular and Celluar BioDiscovery Research Program (2004-01711), and the Center for Molecular Design and Synthesis at KAIST.

## REFERENCES

1. Eddy,S.R. (2001) Non-coding RNA genes and the modern RNA world. *Nature Rev. Genet.*, **2**, 919–920.
2. Gottesman,S. (2004) The small RNA regulators of *Escherichia coli*: roles and mechanisms. *Annu. Rev. Microbiol.*, **58**, 303–328.

3. Storz,G., Opdyke,J.A. and Zhang,A. (2004) Controlling mRNA stability and translation with small, noncoding RNAs. *Curr. Opin. Microbiol.*, **7**, 140–144.
4. Wassarman,K.M. (2002) Small RNAs in bacteria: diverse regulators of gene expression in response to environmental changes. *Cell*, **109**, 141–144.
5. Deutscher,M.P. (1993). RNA maturation nucleases. In Linn,S.M., Lloyd,R.S. and Roberts,R.J. (eds), *Nucleases*. Cold Spring Harbor Laboratory Press, Plainview, NY, pp. 377–406.
6. Deutscher,M.P. (1995) tRNA processing nucleases. In Söll,D. and Rajhandary,U.L. (eds), *tRNA Structure, Biosynthesis and Function*. ASM Press, Washington DC, pp. 51–65.
7. Srivastava,A.K. and Schlessinger,D. (1990) Mechanism and regulation of bacterial ribosomal RNA processing. *Annu. Rev. Microbiol.*, **44**, 105–129.
8. Altman,S. (1989) Ribonuclease P: an enzyme with a catalytic RNA subunit. *Adv. Enzymol. Relat. Areas Mol. Biol.*, **62**, 1–36.
9. Guerrier-Takada,C., Gardiner,K., Marsh,T., Pace,N. and Altman,S. (1983) The RNA moiety of ribonuclease P is the catalytic subunit of enzyme. *Cell*, **35**, 849–857.
10. Lee,Y., Ramamoorthy,R., Park,C.-U. and Schmidt,F.J. (1989) Sites of initiation and pausing in the *Escherichia coli rnpB* (M1 RNA) transcripts. *J. Biol. Chem.*, **264**, 5098–5103.
11. Motamedi,H., Lee,Y. and Schmidt,F.J. (1984) Tandem promoters preceding the gene for the M1 RNA component of *Escherichia coli* ribonuclease P. *Proc. Natl Acad. Sci. USA*, **81**, 3959–3963.
12. Reed,R.E., Baer,M.F., Guerrier-Takada,C., Donis-Keller,H. and Altman,S. (1982) Nucleotide sequence of the gene encoding the RNA subunit (M1 RNA) of ribonuclease P from *Escherichia coli*. *Cell*, **30**, 627–636.
13. Kim,S., Kim,H., Park,I. and Lee,Y. (1996) Mutational analysis of RNA structures and sequences postulated to affect 3′ processing of M1 RNA, the component of *Escherichia coli* RNase P. *J. Biol. Chem.*, **271**, 19330–19337.
14. Li,Z., Pandit,S. and Deutscher,M.P. (1998) 3′ exoribonucleolytic trimming is a common feature of the maturation of small, stable RNAs in *Escherichia coli*. *Proc. Natl Acad. Sci. USA*, **95**, 2856–2861.
15. Lundberg,U. and Altman,S. (1995) Processing of the precursor to the catalytic RNA subunit of RNase P from *Escherichia coli*. *RNA*, **1**, 327–334.
16. Sim,S., Kim,K. and Lee,Y. (2002) 3′-end processing of precursor M1 RNA by the N-terminal half of RNase E. *FEBS Lett.*, **529**, 225–231.
17. Karzai,A.W., Roche,E.D. and Sauer,R.T. (2000) The SsrA-SmpB system for protein tagging, directed degradation and ribosome rescue. *Nature Struct. Biol.*, **1**, 449–455.
18. Komine,Y., Kitabatake,M., Yokogawa,T., Nishikawa,K. and Inokuchi,H.A. (1994) A tRNA-like structure is present in 10Sa RNA, a small stable RNA from *Escherichia coli*. *Proc. Natl Acad. Sci. USA*, **91**, 9223–9227.
19. Lin-Chao,S., Wei,C.L. and Lin,Y.T. (1999) RNase E is required for the maturation of *ssrA* RNA and normal *ssrA* RNA peptide-tagging activity. *Proc. Natl Acad. Sci. USA*, **96**, 12406–12411.
20. Srivastava,R.K., Miczak,A. and Apirion,D. (1990) Maturation of precursor 10Sa RNA in *Escherichia coli* is a two-step process: the first reaction is catalyzed by RNase III in presence of $Mn^{2+}$. *Biochimie*, **72**, 791–802.
21. Hindley,J. (1967) Fractionation of $^{32}$P-labelled ribonucleic acids on polyacrylamide gels and their characterization by fingerprinting. *J. Mol. Biol.*, **30**, 125–136.
22. Lee,S.Y., Bailey,S.C. and Apirion,D. (1978) Small stable RNAs from *Escherichia coli*: evidence for the existence of new molecules and for a new ribonucleoprotein particle containing 6S RNA. *J. Bacteriol.*, **133**, 1015–1023.
23. Lee,C.A., Fournier,M.J. and Beckwith,J. (1985) *Escherichia coli* 6S RNA is not essential for growth or protein secretion. *J. Bacteriol.*, **161**, 1162–1170.
24. Hsu,L.M., Zagorski,J., Wang,Z. and Fournier,M.J. (1985) *Escherichia coli* 6S RNA gene is part of a dual-function transcription unit. *J. Bacteriol.*, **161**, 1162–1170.
25. Wassarman,K.M. and Storz,G. (2000) 6S RNA regulates *E.coli* RNA polymerase activity. *Cell*, **101**, 613–623.
26. Trotochaud,A.E. and Wassarman,K.M. (2004) 6S RNA function enhances long-term cell survival. *J. Bacteriol.*, **186**, 4978–4985.
27. Griffin,B.E. and Baillie,D.L. (1973) Precursors of stable RNA accumulated in a mutant of *E.coli*. *FEBS Lett.*, **34**, 273–279.
28. Babitzke,P., Granger,L., Olszewski,J. and Kushner,S.R. (1993) Analysis of mRNA decay and rRNA processing in *Escherichia coli* multiple mutants carrying a deletion in RNase III. *J. Bacteriol.*, **175**, 229–239.
29. Wachi,M., Umitsuki,G. and Nagai,K. (1997) Functional relationship between *Escherichia coli* RNase E and the CafA protein. *Mol. Gen. Genet.*, **253**, 515–519.
30. Yu,D., Ellis,H.M., Lee,E., Jenkins,N.A., Copeland,N.G. and Court,D.L. (2000) An efficient recombination system for chromosome engineering in *Escherichia coli*. *Proc. Natl Acad. Sci. USA*, **97**, 5978–5983.
31. Rajukumari,K. and Gowrishankar,J. (2002) An N-terminally truncated RpoS (sigma(S)) protein in *Escherichia coli* is active *in vivo* and exhibits normal environmental regulation even in the absence of *rpoS* transcriptional and translational control signals. *J. Bacteriol.*, **184**, 3167–3175.
32. Argaman,L., Hershberg,R., Vogel,J., Bejerano,G., Wagner,E.G.H., Margalit,H. and Altuvia,S. (2001) Novel small RNA encoding genes in the intergenic regions of *Escherichia coli*. *Curr. Biol.*, **11**, 941–950.
33. Lee,Y. and Schmidt,F.J. (1985) Characterization of *in vivo* RNA product of the pOUT promoter of IS10R. *J. Bacteriol.*, **164**, 556–562.
34. Park,J.W., Jung,Y., Lee,S.J., Ding,J.J. and Lee,Y. (2002) Alteration of stringent response of the *Escherichia coli rnpB* promoter by mutations in the −35 region. *Biochem. Biophys. Res. Commun.*, **290**, 1183–1187.
35. Jung,Y.H. and Lee,Y. (1997) *Escherichia coli rnpB* promoter mutants altered in stringent response. *Biochem. Biophys. Res. Commun.*, **230**, 582–586.
36. Buttner,M.J., Smith,A.M. and Bibb,M.J. (1988) At least three different RNA polymerase holoenzymes direct transcription of the agarase gene (*dagA*) of *Streptomyces coelicolor* A3(2). *Cell*, **52**, 1349–1360.
37. Sambrook,J. and Russell,D.W. (2001) *Molecular Cloning: A Laboratory Manual, 3rd edn*. Cold Spring Harbor Laboratory Press, Cold Spring Harbor, NY.
38. Markarov,E.M. and Apirion,D. (1992) 10Sa RNA: processing by and inhibition of RNase III. *Biochem. Int.*, **26**, 1115–1124.
39. Aldea,M., Garrido,T., Hernandez-Chico,C., Vicente,M. and Kushner,S.R. (1989) Induction of a growth-phase-dependent promoter triggers transcription of *bolA*, an *Escherichia coli* morphogene. *EMBO J.*, **8**, 3923–3931.
40. Hengge-Aronis,R. (2002) Stationary phase gene regulation: what makes an *Escherichia coli* promoter sigmaS-selective? *Curr. Opin. Microbiol.*, **5**, 591–595.
41. Jishage,M. and Ishihama,A. (1999) Transcriptional organization and *in vivo* role of the *Escherichia coli rsd* gene, encoding the regulator of RNA polymerase sigma D. *J. Bacteriol.*, **181**, 3768–3776.
42. Lacour,S., Kolb,A. and Landini,P. (2003) Nucleotides from −16 to −12 determine specific promoter recognition by bacterial sigmaS-RNA polymerase. *J. Biol. Chem.*, **278**, 39160–39168.
43. McDowall,K.J. and Cohen,S.N. (1996) The N-terminal domain of the *rne* gene product has RNase E activity and is non-overlapping with the arginine-rich RNA-binding site. *J. Mol. Biol.*, **255**, 349–355.
44. Taraseviciene,L., Bjork,G.R. and Uhlin,B.E. (1995) Evidence for an RNA binding region in the *Escherichia coli* processing endoribonuclease RNase E. *J. Biol. Chem.*, **270**, 26391–26398.
45. Ehretsmann,C.P., Carpousis,A.J. and Krisch,H.M. (1992) Specificity of *Escherichia coli* endoribonuclease RNase E: *in vivo* and *in vitro* analysis of mutants in a bacteriophage T4 mRNA processing site. *Genes Dev.*, **6**, 149–159.
46. Deana,A. and Belasco,J.G. (2004) The functions of RNase G in *Escherichia coli* is constrained by its amino acid carboxyl termini. *Mol. Microbiol.*, **51**, 1205–1217.
47. Lee,K., Bernstein,J.A. and Cohen,S.N. (2002) RNase G complementation of *rne* null mutation identified functional interrelationships with RNase E in *Escherichia coli*. *Mol. Microbiol.*, **43**, 1445–1456.
48. McDowall,K.J., Hernandez,R.G., Lin-Chao,S. and Cohen,S.N. (1993) The *ams-1* and *rne-3071* temperature-sensitive mutations in the *ams* gene are in close proximity to each other and cause substitutions within a domain that resembles a product of the *Escherichia coli mre* locus. *J. Bacteriol.*, **175**, 4245–4249.
49. Okada,Y., Wachi,M., Hirata,A., Suzuki,K., Nagai,K. and Matsuhashi,M. (1994) Cytoplasmic axial filaments in *Escherichia coli* cells: possible

function in the mechanism of chromosome segregation and cell division. *J. Bacteriol.*, **176**, 917–922.
50. Cruz-Reyes,J., Piller,K.J., Rusche,L.N., Mukherjee,M. and Sollner-Webb,B. (1998) Unexpected electrophoretic migration of RNA with different 3′ termini causes a RNA sizing ambiguity that can be resolved using nuclease P1-generated sequencing ladders. *Biochemistry*, **37**, 6059–6064.
51. Jiang,X., Diwa,A. and Belasco,J.G. (2000) Regions of RNase E important for 5′-end-dependent RNA cleavage and autoregulated synthesis. *J. Bacteriol.*, **182**, 2468–2475.
52. Mackie,G.A. (1998) Ribonuclease E is a 5′-end-dependent endonuclease. *Nature*, **395**, 720–723.
53. Tock,M.R., Walsh,A.P., Carroll,G. and McDowall,K.J. (2000) The CafA protein required for the 5′-maturation of 16S rRNA is a 5′-end-dependent ribonuclease that has context-dependent broad sequence specificity. *J. Biol. Chem.*, **275**, 8726–8732.
54. Kaga,N., Umitsuki,G., Nagai,K. and Wachi,M. (2002) RNase G-dependent degradation of the *eno* mRNA encoding a glycolysis enzyme enolase in *Escherichia coli*. *Biosci. Biotechnol. Biochem.*, **66**, 2216–2220.
55. Umitsuki,G., Wachi,M., Takada,A., Hikichi,T. and Nagai,K. (2001) Involvement of RNase G in *in vivo* mRNA metabolism in *Escherichia coli*. *Genes Cells*, **6**, 403–410.
56. Wachi,M., Umitsuki,G., Shimizu,M., Takada,A. and Nagai,K. (1999) *Escherichia coli cafA* gene encodes a novel RNase, designated as RNase G, involved in processing of the 5′ end of 16S rRNA. *Biochem. Biophys. Res. Commun.*, **259**, 483–488.
57. Hershberg,R., Altuvia,S. and Magalit,S. (2003) A survey of small RNA-encoding genes in *Escherichia coli*. *Nucleic Acids Res.*, **31**, 1813–1820.
58. Massé,E., Majdalani,N. and Gottesman,S. (2003) Regulatory roles for small RNAs in bacteria. *Curr. Opin. Microbiol.*, **6**, 120–124.